

Bulletin of Earthquake Engineering manuscript No.
(will be inserted by the editor)

High-frequency filtering of strong-motion records

John Douglas · David M. Boore

Received: date / Accepted: date

Abstract The influence of noise in strong-motion records is most problematic at low and high frequencies where the signal to noise ratio is commonly low compared to that in the mid-spectrum. The impact of low-frequency noise (< 1 Hz) on strong-motion intensity parameters such as ground velocities, displacements and response spectral ordinates can be dramatic and consequentially it has become standard practice to low-cut (high-pass) filter strong-motion data with corner frequencies often chosen based on the shape of Fourier amplitude spectra and the signal-to-noise ratio. It has been shown that response spectral ordinates should not be used beyond some fraction of corner period (reciprocal of the corner frequency) of the low-cut filter. This article examines the effect of high-frequency noise (> 5 Hz) on computed pseudo-absolute response spectral accelerations (PSAs). In contrast to the case of low-frequency noise our analysis shows that filtering to remove high-frequency noise is only necessary in certain situations and that PSAs can often be used up to 100 Hz even if much lower high-cut corner frequencies are required to remove the noise. This apparent contradiction can be explained by the fact that PSAs are often controlled by ground accelerations associated with much lower frequencies than the natural frequency of the oscillator because path and site attenuation (often modelled by Q and κ , respectively) have removed the highest frequencies. We demonstrate that if high-cut filters are to be used, then

J. Douglas

Earthquake Engineering Research Centre, University of Iceland, Austurvegur 2A, Selfoss, IS-800, Iceland
and RNSC/RIS, BRGM, 3 avenue Claude-Guillemin, BP 36009, 45060 Orléans Cedex 2, France

D. M. Boore

US Geological Survey, Mail Stop 977, 345 Middlefield Road, Menlo Park, CA 94025, USA

their corner frequencies should be selected on an individual basis, as has been done in a few recent studies.

Keywords strong-motion data · ground-motion prediction equations · ground-motion models · filtering · response spectra · stochastic method · κ

1 Introduction

In the past decade with the growing interest in displacement-based design and analysis (e.g. Fajfar, 1999; Bommer and Elnashai, 1999; Priestley et al, 2007) and with near-source digital recording of a number of large earthquakes (e.g. 1999 Chi-Chi), many articles have been published discussing the processing of strong-motion records to obtain reliable ground displacements and long-period (> 2 s) response spectral displacements (SDs) (e.g. Boore, 2001, 2004; Akkar and Bommer, 2006; Jousset and Douglas, 2007; Paolucci et al, 2008; Rupakhety et al, 2010). In contrast, the processing of accelerograms to obtain reliable short-period (high-frequency) ($T < 0.1$ s, $f_{osc} > 10$ Hz) spectral accelerations has not received much recent attention. However, the design and analysis of non-structural elements, equipment and pipework (e.g., in nuclear power plants) requires predictions of earthquake ground motions up to high frequencies (e.g. US Nuclear Regulatory Commission, 2007, 2008) and, consequently, a number of recent ground-motion prediction equations (GMPEs) present coefficients to predict pseudo-absolute response spectral accelerations (PSAs) up to 100 Hz (e.g. Power et al, 2008).

During the era of analogue accelerographs (e.g. Kinematics SMA-1) an active topic of research was the processing of strong-motion records to remove the effect of instrument response, which affects high-frequency measurements from such instruments (e.g. Trifunac, 1972). However, correction for instrument response for records from these instruments leads to magnifications of high-frequency noise that then needs to be filtered out since it can dominate the signal (e.g. Converse and Brady, 1992). Time series from digital accelerometers generally do not require adjustment for instrument response because either such instruments already correct for their own response or the instrument has such a high natural frequency (> 50 Hz) that such a correction is deemed not necessary. Records from such instruments, however, usually contain high-frequency noise, particularly if the analogue-to-digital converter (ADC) has a low (10 or 12 bit) resolution or they are located at sites affected by ambient (cultural), wind or wave sources of noise (Figure 1). In addition, some strong-motion

stations are affected by mono-harmonic high-frequency noise, which can be caused by proximity to electrical generators or vibrating machinery (Figure 2). For these two examples the high-frequency PSAs are not greatly affected by the noise, even though it is quite noticeable in their Fourier amplitude spectra (FAS). However, it is important to know when this is the case; when records need to be high-cut filtered (and how to select the corner frequencies of the filters); and when the noise is too great and the data must be rejected. Unfortunately, as noted above, there is little guidance in the literature on what processing should be applied and its effect on obtained response spectral accelerations.

Records with poor high-frequency signal-to-noise ratios are likely to be those with low amplitudes, i.e. from small earthquakes and/or long distances. Therefore, it could be argued that the appropriate processing of such records is of limited interest for engineering purposes. However, when deriving GMPEs it is important that the datasets used are not biased by only including those records that are of higher than average amplitudes, which would be the case if only records with high signal-to-noise ratios were selected. This is a similar situation to not accounting for untriggered instruments when conducting regression analysis (e.g. Bragato, 2004). Hence, extraction of reliable ground-motion parameters from noisy records, even if they come from small earthquakes or large distances, is necessary.

The aim of this article is to present examples of high-cut filtering and its effect on PSAs and give guidance on such filtering, in particular of records from digital instruments. In addition, we assess the impact of not applying high-cut filtering on noisy records because, contrary to what would be expected, high-cut filtering is not always required or desirable even for noisy records. The article begins with a brief review of previous recent work on this topic. Following this some examples of the effect on computed PSAs of filtering of records (both real and simulated) affected by different levels of noise (both real and simulated) from sites with high and low κ (e.g. Anderson and Hough, 1984) are shown. The article ends with some guidance on high-frequency filtering. In the following, since we are interested in high-frequency PSAs, most spectra start at 5 Hz and end at 100 Hz (the highest frequency generally considered in engineering seismology). All PSAs considered here are for linear elastic systems and a critical damping ratio of 5%.

[Fig. 1 about here.]

[Fig. 2 about here.]

2 Previous studies

The Basic strong-motion Accelerogram Processing (BAP) software written by the USGS (Converse and Brady, 1992) or derivatives are commonly used for the routine filtering of acceleration time series. This software includes a routine (HICUT) for high-cut filtering using a cosine half-bell taper in the frequency domain [this is applied after the instrument correction subroutine (INSCOR) for analogue records]. Guidance in the BAP manual (Converse and Brady, 1992) on the frequencies to be used for the filter transition (roll-off and cut-off) of this filter is limited. The default values are: 50–100Hz for digitally-recorded records and for records that were digitized by the automatic trace-following laser digitizer employed by the USGS; and 15–20Hz for manually digitized records. However, it is noted that the ‘50-to-100Hz transition will be too high for many records ... [and] ... the 15-to-20Hz transition will be unnecessarily low for other records. Consequently, the user should either indicate the transition band explicitly ... or carefully consider whether the default provided by the software is appropriate’ (Converse and Brady, 1992). Converse and Brady (1992) present some examples showing the importance of choosing appropriate filter transitions for analogue records on which the noise has been magnified by correction for instrument response. In this article only records from instruments not requiring instrument correction are considered and consequently the examples from Converse and Brady (1992) are of little relevance here.

The recommendations of Converse and Brady (1992) influenced the decision of Ambraseys et al (2005), when deriving GMPEs based on European and Middle Eastern data, to use uniform transitions of 23–25Hz for analogue records (following instrument correction) and 50–100Hz for digital records (without instrument correction) irrespective of the high-frequency noise. GMPEs were derived by Ambraseys et al (2005) for peak ground acceleration (PGA) and spectral accelerations (SAs) for $T \geq 0.05$ s ($f \leq 20$ Hz); a period range that was chosen based on the high-cut filters used. The high-cut filtering applied may influence the predictions for PGA and SA for periods less than 0.1 s but, as shown below, the effect is unlikely to be strong because the generally high κ in the active regions providing the data used by Ambraseys et al (2005) means that there is little energy in the strong-motion data at frequencies above 10Hz. Table 1 presents the highest frequencies for which GMPEs were derived for various models and the reasons (when known) why higher frequencies were not considered [see also Section 5 of Douglas (2003a)]. This table shows

that worries over the accurate recovery of high-frequency PSAs from filtered strong-motion records influenced the authors' decisions on the highest frequency for which to provide equations. It also shows that considerable interpolation between GMPEs for PGA and those for high-frequency PSAs is often required, which brings with it uncertainty in deciding on a frequency to associate with PGA.

[Table 1 about here.]

Boore and Bommer (2005) provide an overview of techniques for processing strong-motion data. They briefly discuss high-cut filtering but their main focus is on long-period motions. They show examples (their Figure 6) contrasting the high-frequency content of strong-motion records from sites with a low κ (with significant high-frequency motions) and sites with a high κ (for which any high-frequency motions have been attenuated by the travel path). They also discuss the importance of the Nyquist frequency (equal to half the sampling rate of the data) beyond which motions cannot be measured.

When processing strong-motion data for the Next Generation Attenuation (NGA) database the cut-off frequencies of both low- and high-cut filters were selected by visual inspection of each time series and associated FAS (Darragh et al, 2004; Chiou et al, 2008). This is unusual, as the individual selection of high-cut filters has not generally been standard practice in processing strong-motion data, for even if care is taken in the choice of low-cut filters, uniform high-cut filters are often employed (e.g. Ambraseys et al, 2005). After filtering acceleration time series for the NGA database, the PSAs were computed up to 100Hz even if the high-cut filter applied had a much lower corner frequency (this is in contrast to low-cut filtering for which a lowest usable frequency was reported). For example, even some recent digital records were high-cut filtered with frequencies less than 10Hz (NGA Flatfile 7.3, peer.berkeley.edu/products/nga_flatfiles_dev.html) but PSAs were used from these records up to 100Hz by the NGA developers.

High-frequency noise levels on some high-quality strong-motion data recorded on 24 bit instruments are sufficiently low that high-frequency filtering is not required (Figure 3). However, low noise is uncommon and consequently the level of the high-frequency noise should be considered if PGAs and PSAs above 10Hz are of interest — the following sections discuss this. Figure 3 demonstrates the danger in applying high-cut filters to records from stations with low κ values because there is considerable high-frequency energy present, which would be removed by standard filtering; this issue is discussed below. For this record there

is little indication of natural attenuation of the ground motion at frequencies as high as 40 to 50 Hz, and therefore the high-cut anti-aliasing filter in the instrument has probably distorted the true PSA at high frequencies. The Nyquist frequency for this record is 62.5 Hz, but if the sample rate for this recording had been much higher it is likely that PSA at high frequencies would have been different than shown in the figure. On the other hand, Figure 3 shows that variations in PSA occur at frequencies well above the Nyquist frequency of 62.5 Hz. There is no inconsistency here, for the PSAs at oscillator frequencies near 100 Hz are being determined by lower frequencies in the input record (in this case, the lack of high-frequency motion in the input record is due either to the applied high-cut filters or the instrumental anti-aliasing high-cut filter).

[Fig. 3 about here.]

3 Effect of high-frequency noise on PSAs

The example of the noisy record with high κ [about 0.06 s based on inspection of a linear-log plot of the Fourier amplitude spectrum, following Anderson and Hough (1984)] presented on Figure 1 shows that although the noise dominates above 20 Hz on the Fourier amplitude spectrum it does not have an effect on the response spectrum. In addition, high-cut filtering does not greatly affect the PSAs. This section investigates when this behaviour can be expected.

The effect of high-frequency filtering on PSAs for records with different noise corner frequencies (f_n) is demonstrated by Figure 4. This figure shows the effect of filters of different f_c on PSAs with oscillator frequencies (f_{osc}) less than and greater than f_n . The PSAs are for the records shown in Figures 1 and 2, for which f_n s of 22 Hz and 48 Hz are estimated (see FAS shown in the original figures). Of particular relevance is the relation of f_{osc} and f_c to f_n , rather than the absolute values of the frequencies. For this reason we plot the PSA ratios against the normalized frequency f_c/f_n . The PSA ratios from both records approach unity (i.e., the PSAs are unaffected by the filtering) when f_c is greater than about half f_n (corresponding to about 11 Hz and 24 Hz for the records shown in Figures 1 and 2 respectively), but if smaller f_c than f_n were used PSA would be significantly underestimated, even for high-frequency oscillators. This is because the oscillator response is being controlled by lower-frequency motions, and filtering at a frequency less than the noise corner is clearly removing signal from the record. This shows the importance of not using a standard f_c for

all records (e.g., 20Hz in Figure 2) but individually choosing f_c for a given record based on its FAS.

[Fig. 4 about here.]

3.1 Simulated time series

The previous examples show that the high-frequency energy content of the strong-motion record can have a significant influence on whether high-cut filtering will have a significant impact on the derived PSAs. For close source-to-site distances this energy content is mainly influenced by κ , which is commonly believed to be mainly related to attenuation in the upper few kilometres of the crust (e.g. Anderson and Hough, 1984). To enable a parametric analysis of the influence of κ and noise levels on PSAs computed before and after high-cut filtering we decided to use ground-motion simulations computed using the stochastic method (e.g. Boore, 2003b) with the addition of simulated noise.

Ground-motion simulations were conducted using a stochastic model for western North America (WNA) with a single-corner-frequency model and a stress parameter $\Delta\sigma$ of 70bar and $\kappa = 0.04$ s. Simulated accelerograms were obtained with no added noise and with white noise added with amplitudes between 1 and 16 gal (cm/s^2) (these amplitudes were chosen to give high-frequency noise levels in FAS that are up to a factor of 100 times smaller than the maximum levels of the FAS). To obtain smooth spectra, the average Fourier amplitude and pseudo-spectral acceleration spectra were computed from many time-domain simulations for each noise level. In addition, simulations were conducted using the stochastic model of Atkinson and Boore (2006) for eastern North America (ENA) for hard rock site conditions, $\kappa = 0.005$ s, and a stress parameter $\Delta\sigma$ of 210bar, which is close to the geometric mean stress parameter determined for eight relatively well-recorded earthquakes in ENA (Boore et al, 2010).

In addition to noise from ambient (cultural) sources, wind and electronic noise, high-frequency noise in digital records can also be produced during the ADC process; this can be particularly important for instruments with low resolution (10 or 12 bit). This source of noise has been discussed and its effect on derived strong-motion intensity parameters has been evaluated by Douglas (2003b) and Boore (2003a). Douglas (2003b) found that if an accelerogram contains more than about ten acceleration levels then accurate SAs between 0.2 and 2s could be obtained. Boore (2003a) found that ADC can produce apparent changes

in the acceleration baseline leading to low-order polynomial trends that can be seen in velocity and displacement time series derived by integration; this effect is most pronounced for low-resolution ADC. It is straightforward to simulate this type of noise since all that is required is to round the ground acceleration to the acceleration corresponding to the nearest bit level (based on the bit range and full-scale amplitude of the simulated instrument); but, because its effect has been discussed previously, we do not consider it in this article.

3.2 Effects of noise and filtering on high-frequency response spectra

The simulated data were filtered using causal Butterworth filters with a high-frequency response of $(f_c/f)^6$, where f_c is the corner frequency. The filter was chosen to approximate the one most commonly used to process the records in the PEER NGA flatfile. Similar results could be obtained using a cosine half-bell filter such as employed by BAP (Converse and Brady, 1992) if its cut- and roll-off frequencies were chosen appropriately to match the gain of this causal Butterworth filter. Firstly to study the effect of uniform cut-offs, as are often used in practice, corner frequencies of 10, 20 and 40Hz were chosen. However, these corner frequencies do not account for the noise levels. Therefore, corner frequencies equal to the frequency f_n where a line through the high-frequency noise on a FAS plot (the flat part of the spectrum) intersects a straight-line fit (on a log-log plot) to the decay of the FAS before reaching the noise floor (below which no signal can be measured) were also selected (see Figure 5). These corner frequencies would be similar to those chosen by applying the NGA processing procedure mentioned above. These corner frequencies vary with the signal-to-noise ratio. For example, for simulations of a **M** 6.5 earthquake at 30km the corner frequency chosen by this approach varies from 19Hz for a noise level of 16gal to 36Hz for a noise level of 1 gal. The computed FAS for the WNA and ENA stochastic models are shown in Figures 5 and 6, respectively.

[Fig. 5 about here.]

[Fig. 6 about here.]

PSAs were computed from the simulations. To better see the effect of the noise and the filtering on the PSAs the ratios of the PSAs from the records with noise (without and with filtering) to the PSAs from the noise-free records were calculated (Figures 7 and 8).

[Fig. 7 about here.]

[Fig. 8 about here.]

High-frequency PSAs can be controlled by frequencies much lower than the frequency of the oscillator. For example, PSAs at 100Hz can be controlled by accelerations at 10Hz. Analysis of the NGA Flatfile shows that PGA is generally less than 2% lower than PSA(100Hz) (e.g. Idriss, 2007), although for hard-rock sites with very low κ s close to the earthquake source this may not always be true. The presence of noise between the frequencies controlling the PSAs and the frequency of the oscillator may not be important. To summarize this effect the ratio between the peak high-frequency Fourier amplitude and the Fourier amplitude in the flat portion at high frequencies was computed and plotted against the maximum ratio of the PSAs with noise (unfiltered and filtered) to the noise-free PSAs (Figure 9). For example, for the WNA simulations the ratios between a representative maximum Fourier amplitudes and the noise floors are estimated from Figure 5 (e.g. $17/4.2 = 4.0$ for the 16 gal simulations), which are plotted against the ratio of PSAs with and without noise obtained from Figure 7 (e.g. about 1.5 for the 16 gal simulations). Figure 9 allows an estimate to be made of when noise levels start to swamp the signal and thereby affect PSAs. Note that this figure is for general guidance only and its intention is not to provide exact values of the expected error.

[Fig. 9 about here.]

Figure 9 includes results from both the WNA and ENA simulations. In addition, as a check of the generality of the result, points from a simulation study in which the “true” ground motion was taken to be a filtered version of an actual record with very different magnitude and distance than assumed for the simulated records are displayed. The use of ratios of the maximum Fourier amplitudes and the noise floor and the ratios of PSAs with and without noise *independent* of frequency (i.e. not the ratios at specific frequencies) reduces the influence of the shape of the FAS, which explains the similarity in the results for the WNA and ENA simulations for which the peak ratios occur at much different frequencies, mainly due to differing κ s. Although not identical, the results from the various simulations are in general agreement and provide an estimate of the error in high-frequency PSA computed from records in which no high-cut filters have been applied. For example, the ratio of maximum to noise-floor FAS in Figures 1 and 2 are about 10 and 100 (ignoring the spikes at 50Hz and 78Hz), respectively, from which we estimate from Figure 9 that the error in the PSA for the unfiltered records would be 15% and less than 2%, respectively. In addition,

Figure 1 indicates that the effect of filtering is, as desired, to reduce significantly the influence of the noise, with reliable estimates of PSA at oscillator frequencies much above the high-cut filter corner frequencies.

3.3 Effect of mono-harmonic noise on PSAs

The accelerogram shown in Figure 2 is used as an example of a time series affected by high-frequency mono-harmonic noise, which could be expected for instruments located close to vibrating machinery, for example. Accurate PSAs close to the frequency of the mono-harmonic noise can be obtained after applying a notch (bandstop) filter even though, for this time series, this noise is not significantly affecting the computed PSAs (Figure 10). Notch filters are more appropriate in this case than standard high-cut filters, which do not fully remove the noise at 50Hz and, in addition, affect PSAs at neighbouring frequencies (Figure 10).

[Fig. 10 about here.]

4 Conclusions

In this brief article we have investigated the need for filtering to remove high-frequency noise in strong-motion records based on some example accelerograms and a series of simulations. In contrast to low-cut filtering, for which only SDs at periods lower than some proportion (0.3–0.9 depending on site class, instrument type and tolerance criterion) of the cut-off period are reliable (Akkar and Bommer, 2006), in many situations accurate high-frequency PSAs up to 100Hz can be obtained even in the presence of high noise levels with or without filtering to remove this noise. A useful parameter in determining the probable error in high-frequency PSAs from acceleration time series with no high-cut filtering is the ratio of the FAS near the peak portion of the spectrum to that near the noise floor (assuming a white-noise model); if this ratio is greater than ten, our simulation study shows that the error in PSA will be less than about 15% even without filtering. If relative noise levels are high, it is important that high-cut corner frequencies are chosen individually, based on where the Fourier amplitude spectrum of the signal meets the noise floor. The use of uniform filter corner frequencies (e.g. 25Hz) can lead to incorrect PSAs at high frequencies. Even though

mono-harmonic noise is prominent as spikes on FAS of some accelerograms its impact on PSAs is limited and it can be reduced further by the application of notch (bandstop) filters.

Acknowledgements JD thanks Landsvirkjun and the University of Iceland for his one-year visiting professorship at the Earthquake Engineering Research Centre. The strong-motion networks in France are operated by various organizations (see RAP website), under the aegis of the RAP. The RAP data centre is based at Laboratoire de Géophysique Interne et de Tectonophysique, Grenoble. The Icelandic Strong-Motion Network is operated by the Earthquake Engineering Research Centre, University of Iceland. We are grateful to the personnel of these organizations for operating the stations and providing us with the data. We thank Sinan Akkar, Julian Bommer, Basil Margaris, Roberto Paolucci and Chris Stephens for careful reviews of this article, and Jon Ake and Brian Chiou for providing references.

References

- Abrahamson NA, Silva WJ (1997) Empirical response spectral attenuation relations for shallow crustal earthquakes. *Seismological Research Letters* 68(1):94–127
- Akkar S, Bommer JJ (2006) Influence of long-period filter cut-off on elastic spectral displacements. *Earthquake Engineering and Structural Dynamics* 35(9):1145–1165
- Ambraseys NN, Simpson KA, Bommer JJ (1996) Prediction of horizontal response spectra in Europe. *Earthquake Engineering and Structural Dynamics* 25(4):371–400
- Ambraseys NN, Douglas J, Sarma SK, Smit PM (2005) Equations for the estimation of strong ground motions from shallow crustal earthquakes using data from Europe and the Middle East: Horizontal peak ground acceleration and spectral acceleration. *Bulletin of Earthquake Engineering* 3(1):1–53, DOI 10.1007/s10518-005-0183-0
- Anderson JG, Hough SE (1984) A model for the shape of the Fourier amplitude spectrum of acceleration at high frequencies. *Bulletin of the Seismological Society of America* 74(5):1969–1993
- Atkinson GM, Boore DM (2006) Earthquake ground-motion prediction equations for eastern North America. *Bulletin of the Seismological Society of America* 96(6):2181–2205, DOI 10.1785/0120050245
- Bindi D, Luzi L, Massa M, Pacor F (2010) Horizontal and vertical ground motion prediction equations derived from the Italian Accelerometric Archive (ITACA). *Bulletin of Earthquake Engineering* DOI 10.1007/s10518-009-9130-9, in press

- Bommer JJ, Elnashai AS (1999) Displacement spectra for seismic design. *Journal of Earthquake Engineering* 3(1):1–32
- Boore DM (2001) Effect of baseline corrections on displacements and response spectra for several recordings of the 1999 Chi-Chi, Taiwan, earthquake. *Bulletin of the Seismological Society of America* 91(5):1199–1211
- Boore DM (2003a) Analog-to-digital conversion as a source of drifts in displacements derived from digital recordings of ground acceleration. *Bulletin of the Seismological Society of America* 93(5):2017–2024
- Boore DM (2003b) Simulation of ground motion using the stochastic method. *Pure and Applied Geophysics* 160(3–4):635–676, DOI 10.1007/PL00012553
- Boore DM (2004) Long-period ground motions from digital acceleration recordings: A new era in engineering seismology. In: *Proceedings of the International Workshop on Future Directions in Instrumentation for Strong Motion and Engineering Seismology*, Kluwer, Kusadasi, Turkey
- Boore DM, Atkinson GM (2008) Ground-motion prediction equations for the average horizontal component of PGA, PGV, and 5%-damped PSA at spectral periods between 0.01 s and 10.0 s. *Earthquake Spectra* 24(1):99–138, DOI 10.1193/1.2830434
- Boore DM, Bommer JJ (2005) Processing of strong-motion accelerograms: Needs, options and consequences. *Soil Dynamics and Earthquake Engineering* 25(2):93–115
- Boore DM, Campbell KW, Atkinson GM (2010) Determination of stress parameters for eight well-recorded earthquakes in eastern North America. *Bulletin of the Seismological Society of America* 100(4):1632–1645, DOI 10.1785/0120090328
- Bragato PL (2004) Regression analysis with truncated samples and its application to ground-motion attenuation studies. *Bulletin of the Seismological Society of America* 94(4):1369–1378
- Campbell KW (1997) Empirical near-source attenuation relationships for horizontal and vertical components of peak ground acceleration, peak ground velocity, and pseudo-absolute acceleration response spectra. *Seismological Research Letters* 68(1):154–179
- Chiou B, Darragh R, Gregor N, Silva W (2008) NGA project strong-motion database. *Earthquake Spectra* 24(1):23–44, DOI 10.1193/1.2894831
- Converse AM, Brady AG (1992) BAP basic strong-motion accelerogram processing software, version 1.0. Open-File Report 92-296A, US Geological Survey

-
- Danciu L, Tselentis GA (2007) Engineering ground-motion parameters attenuation relationships for Greece. *Bulletin of the Seismological Society of America* 97(1B):162–183, DOI 10.1785/0120040087
- Darragh B, Silva W, , Gregor N (2004) Strong motion record processing procedures for the PEER center. In: *Proceedings of COSMOS Workshop on Strong-Motion Record Processing*, Richmond, California, pp 1–12
- Douglas J (2003a) Earthquake ground motion estimation using strong-motion records: A review of equations for the estimation of peak ground acceleration and response spectral ordinates. *Earth-Science Reviews* 61(1–2):43–104
- Douglas J (2003b) What is a poor quality strong-motion record? *Bulletin of Earthquake Engineering* 1(1):141–156
- Fajfar P (1999) Capacity spectrum method based on inelastic demand spectra. *Earthquake Engineering and Structural Dynamics* 28(9):979–993
- Idriss IM (2007) Empirical model for estimating the average horizontal values of pseudo-absolute spectral accelerations generated by crustal earthquakes, volume 1 (sites with $v_{s30} = 450$ to 900m/s). Interim report issued for USGS review
- Johnson RA (1973) An earthquake spectrum prediction technique. *Bulletin of the Seismological Society of America* 63(4):1255–1274
- Jousset P, Douglas J (2007) Long-period earthquake ground displacements recorded on Guadeloupe (French Antilles). *Earthquake Engineering and Structural Dynamics* 36(7):949–963, DOI 10.1002/eqe.666
- Joyner WB, Boore DM (1982) Prediction of earthquake response spectra. Open-File Report 82-977, U.S. Geological Survey
- Joyner WB, Boore DM (1988) Measurement, characterization, and prediction of strong ground motion. In: *Proceedings of Earthquake Engineering & Soil Dynamics II*, Geotechnical Division, ASCE, pp 43–102
- Paolucci R, Rovelli A, Faccioli E, Cauzzi C, Finazzi D, Vanini M, Di Alessandro C, Calderoni G (2008) On the reliability of long period spectral ordinates from digital accelerograms. *Earthquake Engineering and Structural Dynamics* 37(5):697–710
- Péquegnat C, Guéguen P, Hatzfeld D, Langlais M (2008) The French Accelerometric Network (RAP) and National Data Centre (RAP-NDC). *Seismological Research Letters* 79(1):79–89

-
- Power M, Chiou B, Abrahamson N, Bozorgnia Y, Shantz T, Roblee C (2008) An overview of the NGA project. *Earthquake Spectra* 24(1):3–21, DOI 10.1193/1.2894833
- Priestley MJN, Calvi GM, Kowalsky MJ (2007) *Displacement-Based Seismic Design of Structures*. IUSS Press, Pavia, Italy, 721pp.
- Rupakhety R, Halldorsson B, Sigbjörnsson R (2010) Estimating coseismic deformations from near source strong motion records: Methods and case studies. *Bulletin of Earthquake Engineering* 8(4):787–811, DOI 10.1007/s10518-009-9167-9
- Sabetta F, Pugliese A (1996) Estimation of response spectra and simulation of nonstationary earthquake ground motions. *Bulletin of the Seismological Society of America* 86(2):337–352
- Sadigh K, Chang CY, Egan JA, Makdisi F, Youngs RR (1997) Attenuation relationships for shallow crustal earthquakes based on California strong motion data. *Seismological Research Letters* 68(1):180–189
- Sylvander M, Souriau A, Rigo A, Tocheport A, Toutain JP, Ponsolles C, Benahmed S (2008) The 2006 November, $M_L = 5.0$ earthquake near Lourdes (France): New evidence for NS extension across the Pyrenees. *Geophysical Journal International* 175(2):649–664, DOI 10.1111/j.1365-246X.2008.03911.x
- Trifunac MD (1972) A note on correction of strong-motion accelerograms for instrument response. *Bulletin of the Seismological Society of America* 62(1):401–409
- Trifunac MD (1978) Response spectra of earthquake ground motions. *Journal of The Engineering Mechanics Division, ASCE* 104(EM5):1081–1097
- US Nuclear Regulatory Commission (2007) A performance-based approach to define the site specific earthquake ground motion. *Regulatory Guide* 1.208
- US Nuclear Regulatory Commission (2008) Interim staff guidance on seismic issues associated with high frequency ground motion in design certification and combined license applications. *Interim Staff Guidance DC/COL-ISG1*
- Zhao JX, Zhang J, Asano A, Ohno Y, Oouchi T, Takahashi T, Ogawa H, Irikura K, Thio HK, Somerville PG, Fukushima Y, Fukushima Y (2006) Attenuation relations of strong ground motion in Japan using site classification based on predominant period. *Bulletin of the Seismological Society of America* 96(3):898–913, DOI 10.1785/0120050122

List of Figures

- 1 Example of strong-motion record featuring significant high-frequency noise (above 22 Hz) and the effect on PSA of applying various high-cut filters. The record is the NS component from the Oseyrarbru station of the Icelandic Strong-Motion Network of the 17th June 2000 (m_b 3.9) Hengill earthquake. Epicentral distance $r_{epi} = 20$ km. a) uncorrected acceleration time series; b) Fourier amplitude spectra (FAS) of signal and pre-event noise (first 5.12 s of record, corrected for duration differences of the event and the noise sample by multiplying the noise FAS by the square root of the ratio of the event and the noise durations); c) PSAs for unfiltered record and PSAs for record filtered using a causal Butterworth frequency with high frequency response going as $(f_c/f)^6$, where $f_c = 20$ Hz and 40 Hz. Note that, in this case, the spectra from the filtered time series are very similar to those from the noisy uncorrected record. Also indicated as thick marks at the right-hand side of this plot are the PGAs read directly from the time series (the PSA are plotted to 200 Hz to capture the high-frequency equivalence of PSA and PGA). . . . 18
- 2 Example of strong-motion record featuring quasi mono-harmonic noise at 50 Hz, with a broader and more subdued noise source near 78 Hz and the effect on PSA of applying various high-cut filters. The quasi mono-harmonic noise is thought to be due to the proximity to electrical generators. A vertical gray line has been added at 50 Hz on the PSA graph to focus on the influence of the 50 Hz noise on the response spectrum and the consequence of high-cut filtering to reduce that noise. The record is the longitudinal component from the station at the Sultartanga-Hydroelectric Power Plant of the Icelandic Strong-Motion Network of the 17th June 2000 (**M** 6.5) South Iceland earthquake. Joyner-Boore distance $r_{jb} = 39$ km. See caption of Figure 1 for details of the subplots; the first 2.56 s was used for the noise sample. Although the equivalence of high-frequency PSA and PGA occurs at a frequency less than 100 Hz, the PSA is plotted to 200 Hz for consistency with Figures 1 and 3. 19

-
- 3 Example of strong-motion record with an excellent signal-to-noise ratio and the effect on PSA of applying various high-cut filters. The record is the EW component from the PYLS (Luz-Saint-Sauveur) hard-rock station of the French accelerometric network (Réseau Accélérométrique Permanent, RAP) (Péquegnat et al, 2008) of the 17th November 2006 (**M** 4.4) normal-faulting earthquake near Lourdes (Sylvander et al, 2008). Epicentral distance $r_{epi} = 19\text{km}$. See caption of Figure 1 for details of the subplots; the first 8.19s was used for the noise sample. The rapid decay in the FAS starting at about 50Hz is thought to be due to the instrumental anti-aliasing filter. The PSA are plotted to 200 Hz to capture the high-frequency equivalence of PSA and PGA. 20
- 4 Ratios of PSAs at oscillator frequencies (f_{osc}) of: a) 10Hz and b) 200Hz from high-frequency filtered, with corner frequencies f_c , and unfiltered records shown in Figures 1 and 2, with f_n s of 22Hz and 48Hz respectively, against f_c/f_n . The ratios of f_{osc} to f_n are given in the graph legends; those in graph a are less than 1 and those in graph b are greater than 1. 21
- 5 Average FAS for 500 noise-added simulations, without and with high-cut filtering (solid and dashed lines, respectively) at the filter corner frequencies indicated by the short vertical lines. The corner frequencies were determined by the intersection of subjectively chosen lines fit to the high-frequency and sloping portions of the FAS, as shown for noise of 4 gals (these frequencies are denoted f_n elsewhere in this paper, so in this figure $f_c = f_n$). Also shown is the FAS for a 40Hz filter for 16gals noise. 22
- 6 Average FAS spectra for 100 unfiltered noise-added simulations for ENA. Note the difference in the frequency axis compared to the previous figure for WNA; this difference is a result of the much lower κ , which results in the peak of the PSA being at higher frequencies than for the WNA simulations. 23
- 7 Ratios of average PSAs from noise-added simulations and noise-free simulations. The thick and thin lines are for unfiltered and filtered simulations, respectively. The two vertical gray lines are plotted at the corner frequencies used for 16 gal and 1 gal added noise (18.8 and 36.3Hz, respectively). . . . 24

-
- 8 Ratios of average response spectra spectra from 100 unfiltered noise-added and noise-free ENA simulations. The Nyquist frequency of these simulations is 500Hz. Note the difference in the frequency axis compared to that used in the corresponding figure for the WNA simulations. The simulations for each noise level used the same random-number seed, and therefore the added noise only changed amplitude, not spectral content; this may explain the similarity of the small fluctuations in PSA with oscillator frequency over the suite of PSAs. 25
 - 9 Ratios of average response spectra from noise-added simulations and noise-free simulations versus ratios of average Fourier spectra near the peak of the FAS, with respect to the high-frequency noise level. 26
 - 10 Fourier spectra and PSAs for the accelerogram shown in Figure 2, without filtering and with a 40Hz high-cut filter and a 50Hz narrow-band rejection (notch) filter (the vertical gray line at 50 Hz in the right-hand graph is drawn at the corner frequency of the notch filter). 27

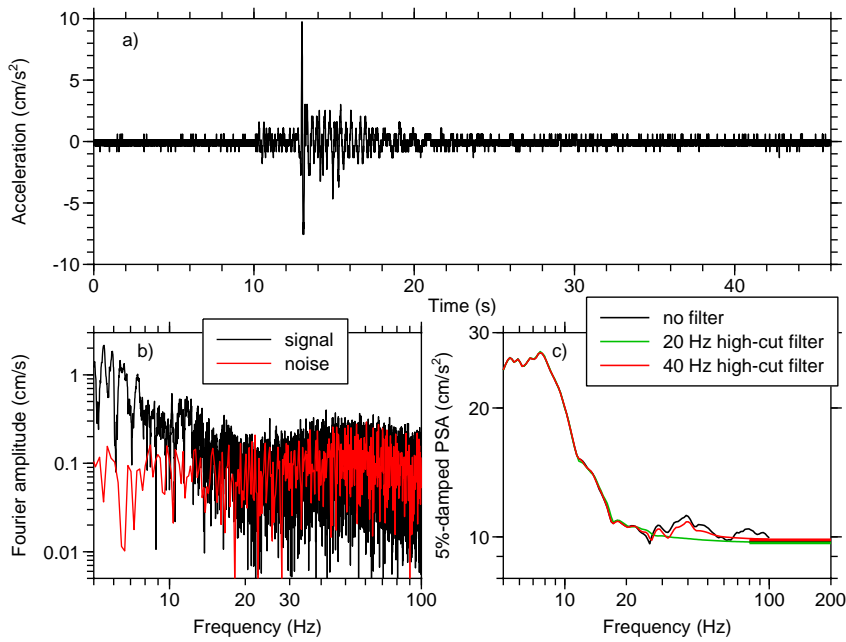


Fig. 1 Example of strong-motion record featuring significant high-frequency noise (above 22 Hz) and the effect on PSA of applying various high-cut filters. The record is the NS component from the Oseyrarbrú station of the Icelandic Strong-Motion Network of the 17th June 2000 ($m_b 3.9$) Hengill earthquake. Epicentral distance $r_{epi} = 20$ km. a) uncorrected acceleration time series; b) Fourier amplitude spectra (FAS) of signal and pre-event noise (first 5.12 s of record, corrected for duration differences of the event and the noise sample by multiplying the noise FAS by the square root of the ratio of the event and the noise durations); c) PSAs for unfiltered record and PSAs for record filtered using a causal Butterworth frequency with high frequency response going as $(f_c/f)^6$, where $f_c = 20$ Hz and 40 Hz. Note that, in this case, the spectra from the filtered time series are very similar to those from the noisy uncorrected record. Also indicated as thick marks at the right-hand side of this plot are the PGAs read directly from the time series (the PSA are plotted to 200 Hz to capture the high-frequency equivalence of PSA and PGA).

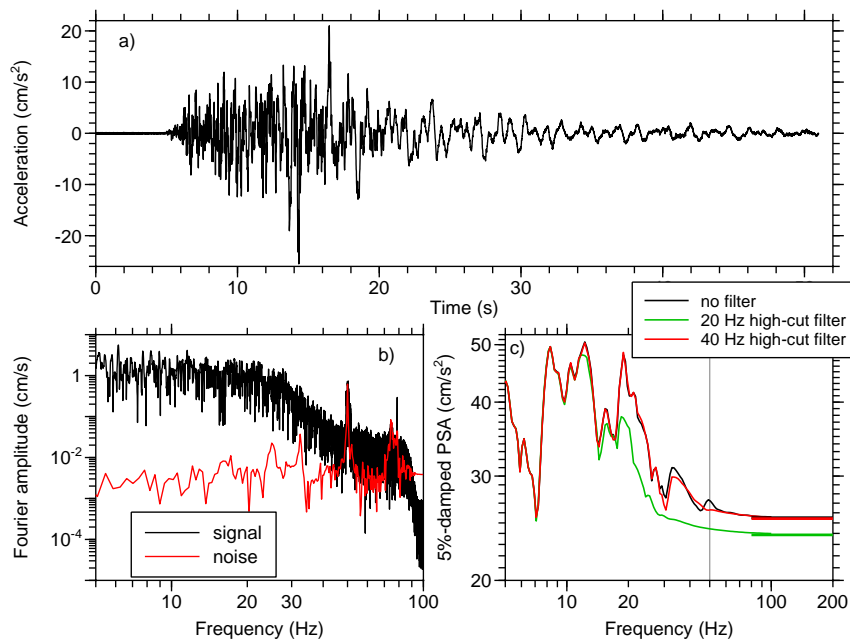


Fig. 2 Example of strong-motion record featuring quasi mono-harmonic noise at 50Hz, with a broader and more subdued noise source near 78Hz and the effect on PSA of applying various high-cut filters. The quasi mono-harmonic noise is thought to be due to the proximity to electrical generators. A vertical gray line has been added at 50 Hz on the PSA graph to focus on the influence of the 50 Hz noise on the response spectrum and the consequence of high-cut filtering to reduce that noise. The record is the longitudinal component from the station at the Sultartanga-Hydroelectric Power Plant of the Icelandic Strong-Motion Network of the 17th June 2000 (M 6.5) South Iceland earthquake. Joyner-Boore distance $r_{jb} = 39$ km. See caption of Figure 1 for details of the subplots; the first 2.56 s was used for the noise sample. Although the equivalence of high-frequency PSA and PGA occurs at a frequency less than 100 Hz, the PSA is plotted to 200 Hz for consistency with Figures 1 and 3.

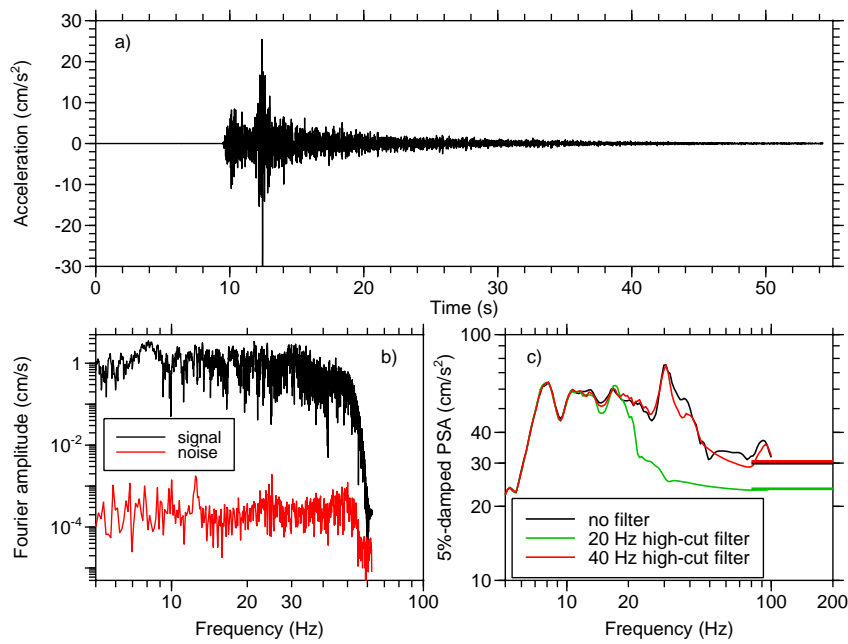


Fig. 3 Example of strong-motion record with an excellent signal-to-noise ratio and the effect on PSA of applying various high-cut filters. The record is the EW component from the PYLS (Luz-Saint-Sauveur) hard-rock station of the French accelerometric network (Réseau Accélérométrique Permanent, RAP) (Péquegnat et al, 2008) of the 17th November 2006 (M 4.4) normal-faulting earthquake near Lourdes (Sylvander et al, 2008). Epicentral distance $r_{epi} = 19$ km. See caption of Figure 1 for details of the subplots; the first 8.19 s was used for the noise sample. The rapid decay in the FAS starting at about 50 Hz is thought to be due to the instrumental anti-aliasing filter. The PSA are plotted to 200 Hz to capture the high-frequency equivalence of PSA and PGA.

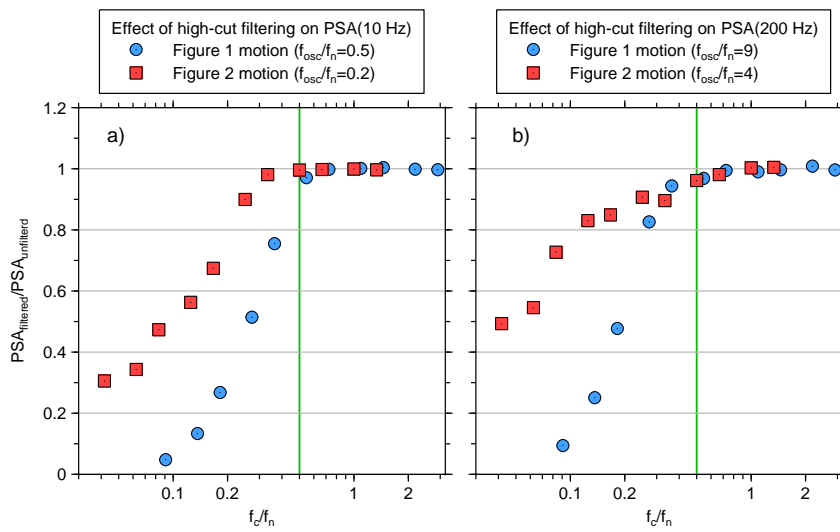


Fig. 4 Ratios of PSAs at oscillator frequencies (f_{osc}) of: a) 10 Hz and b) 200 Hz from high-frequency filtered, with corner frequencies f_c , and unfiltered records shown in Figures 1 and 2, with f_n s of 22 Hz and 48 Hz respectively, against f_c/f_n . The ratios of f_{osc} to f_n are given in the graph legends; those in graph a are less than 1 and those in graph b are greater than 1.

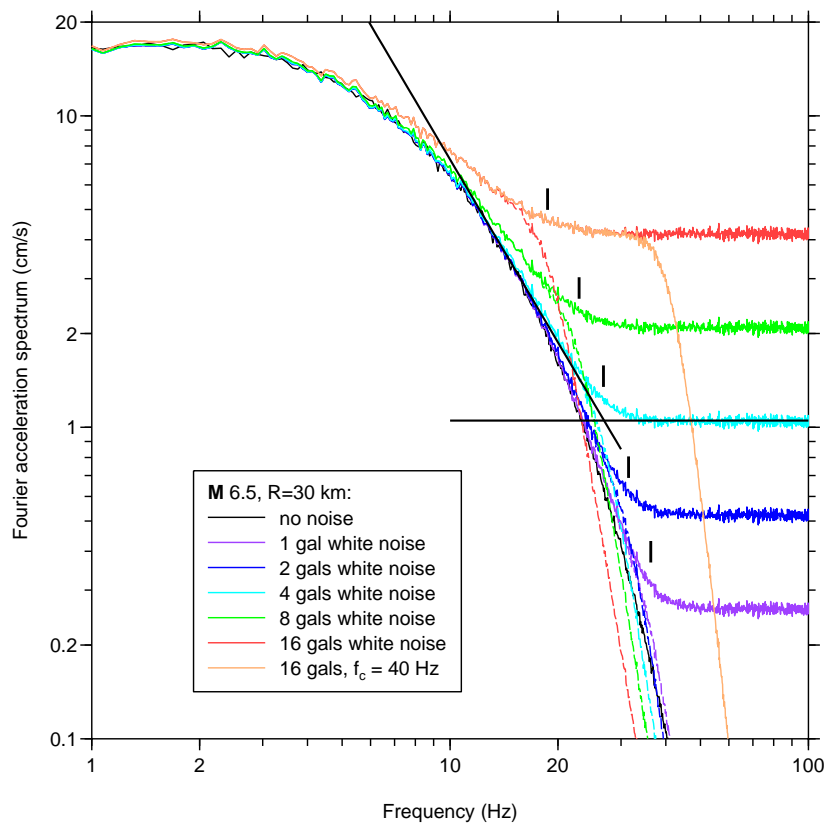


Fig. 5 Average FAS for 500 noise-added simulations, without and with high-cut filtering (solid and dashed lines, respectively) at the filter corner frequencies indicated by the short vertical lines. The corner frequencies were determined by the intersection of subjectively chosen lines fit to the high-frequency and sloping portions of the FAS, as shown for noise of 4 gals (these frequencies are denoted f_n elsewhere in this paper, so in this figure $f_c = f_n$). Also shown is the FAS for a 40 Hz filter for 16 gals noise.

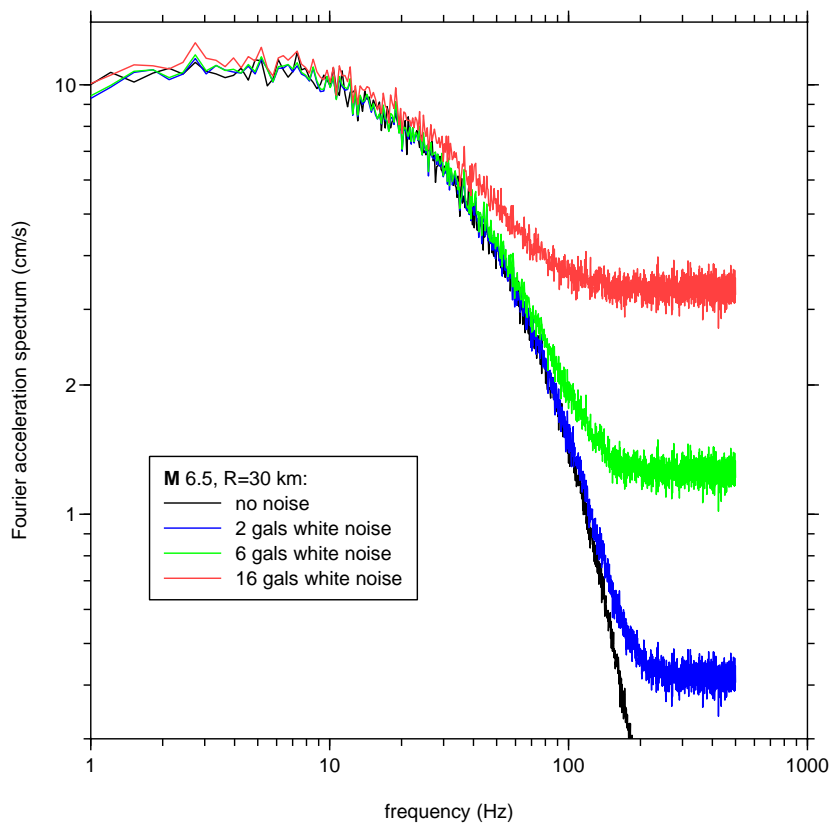


Fig. 6 Average FAS spectra for 100 unfiltered noise-added simulations for ENA. Note the difference in the frequency axis compared to the previous figure for WNA; this difference is a result of the much lower κ , which results in the peak of the PSA being at higher frequencies than for the WNA simulations.

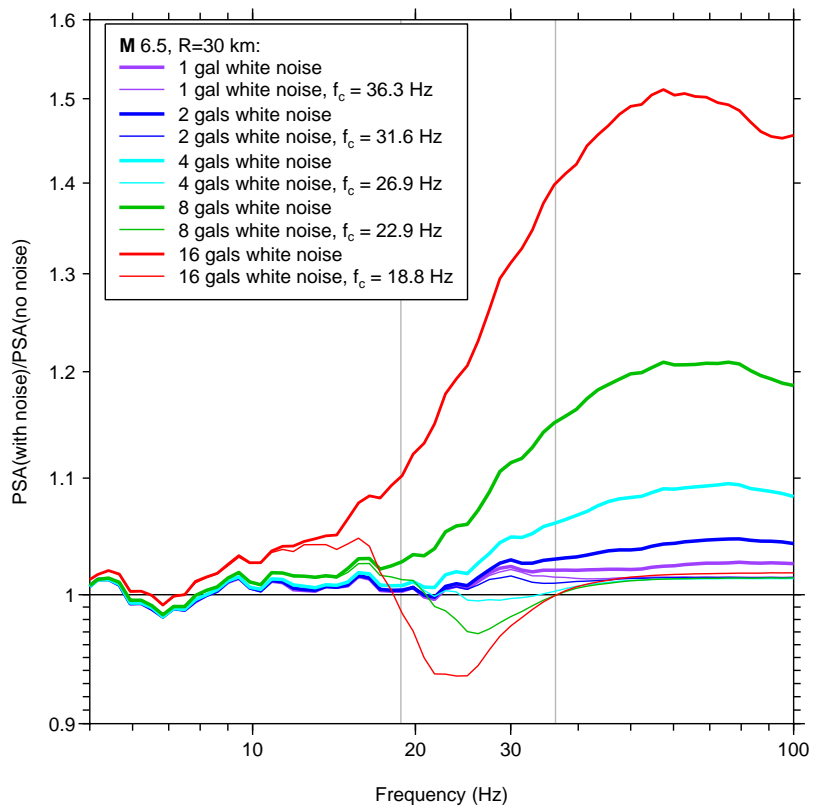


Fig. 7 Ratios of average PSAs from noise-added simulations and noise-free simulations. The thick and thin lines are for unfiltered and filtered simulations, respectively. The two vertical gray lines are plotted at the corner frequencies used for 16 gal and 1 gal added noise (18.8 and 36.3 Hz, respectively).

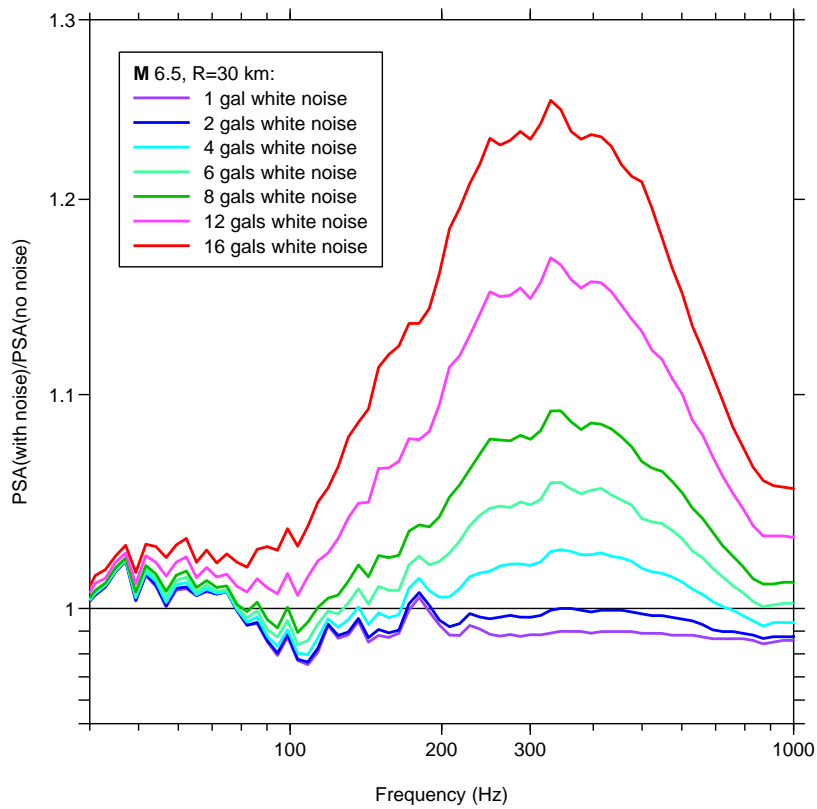


Fig. 8 Ratios of average response spectra spectra from 100 unfiltered noise-added and noise-free ENA simulations. The Nyquist frequency of these simulations is 500Hz. Note the difference in the frequency axis compared to that used in the corresponding figure for the WNA simulations. The simulations for each noise level used the same random-number seed, and therefore the added noise only changed amplitude, not spectral content; this may explain the similarity of the small fluctuations in PSA with oscillator frequency over the suite of PSAs.

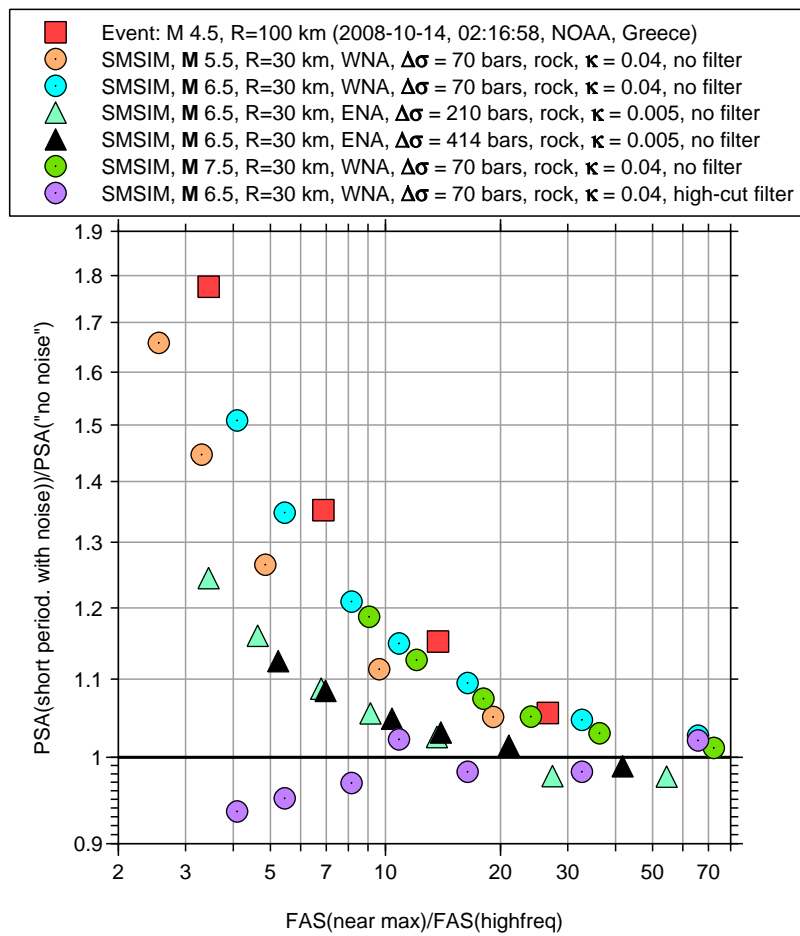


Fig. 9 Ratios of average response spectra from noise-added simulations and noise-free simulations versus ratios of average Fourier spectra near the peak of the FAS, with respect to the high-frequency noise level.

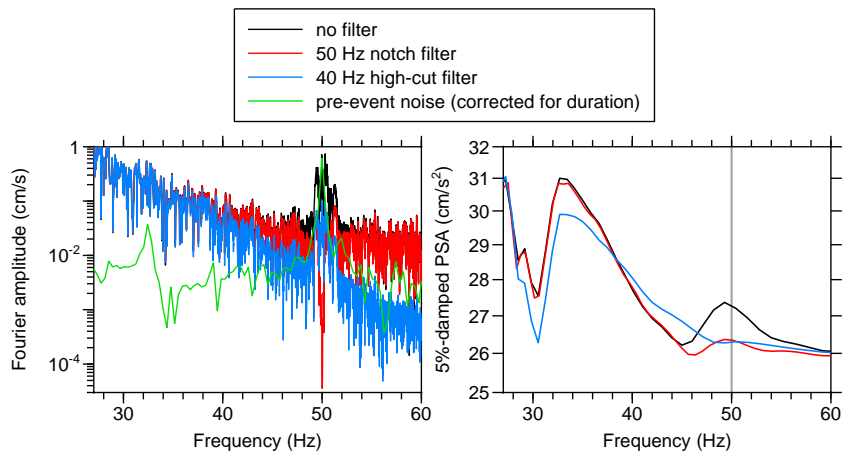


Fig. 10 Fourier spectra and PSAs for the accelerogram shown in Figure 2, without filtering and with a 40Hz high-cut filter and a 50Hz narrow-band rejection (notch) filter (the vertical gray line at 50 Hz in the right-hand graph is drawn at the corner frequency of the notch filter).

List of Tables

- 1 The highest frequencies (f_{osc}) (lowest periods, T) for which various authors presented GMPEs for the prediction of PSA (or SA) and their reasoning (if known). Note that the processing information given in the “Reason” column does not imply that the authors of the GMPE did the processing; in fact, most of the GMPEs used data processed by others. Only GMPEs by Zhao et al (2006) and Boore and Atkinson (2008) in this list were derived using a large number records from digital instruments (the other GMPEs are overwhelmingly based on records from analogue instruments). 29

Table 1 The highest frequencies (f_{osc}) (lowest periods, T) for which various authors presented GMPEs for the prediction of PSA (or SA) and their reasoning (if known). Note that the processing information given in the “Reason” column does not imply that the authors of the GMPE did the processing; in fact, most of the GMPEs used data processed by others. Only GMPEs by Zhao et al (2006) and Boore and Atkinson (2008) in this list were derived using a large number records from digital instruments (the other GMPEs are overwhelmingly based on records from analogue instruments).

Reference	f_{osc} (Hz)	T (s)	Reason
Johnson (1973)	18	0.055	Not known
Trifunac (1978)	25	0.04	Records instrument corrected and high-cut filtered at 25Hz.
Joyner and Boore (1982)	10	0.1	Inaccurate instrument correction above 10 Hz (Joyner and Boore, 1988)
Ambraseys et al (1996)	10	0.1	Records high-cut filtered at 25Hz.
Sabetta and Pugliese (1996)	25	0.04	Records instrument corrected and high-cut filtered with cut-offs between 20 and 35 Hz (most about 25Hz).
Abrahamson and Silva (1997)	100	0.01	Records instrument corrected and high-cut filtered with individually chosen cut-offs, f_h . PSAs only used up to $0.8f_h$ hence less than 100 records used at 100Hz. They assume that PSA(100Hz) equals PGA.
Campbell (1997)	20	0.05	Records high-cut filtered at 25 Hz.
Sadigh et al (1997)	20	0.05	Not known
Zhao et al (2006)	20	0.05	Records instrument corrected and high-cut filtered with cut-offs of either 24.5 Hz (50 samples-per-second data) or 33 Hz (100 samples-per-second data).
Danciu and Tselentis (2007)	10	0.1	Records high-cut filtered at 25 Hz.
Boore and Atkinson (2008)	100	0.01	See text. The other NGA models also present equations up to 100Hz
Bindi et al (2010)	33	0.03	Records instrument corrected and high-cut filtered with cut-offs between roughly 20 (analogue data) and 30 Hz (digital data).